All-optical regenerative NRZ-to-RZ format conversion using coupled ring-resonator optical waveguide

Tong Ye,* Cishuo Yan, Yuanyuan Lu, Fangfei Liu, and Yikai Su

State Key Laboratory of Advanced Optical Communication Systems and Networks, Department of Electronic Engineering, Shanghai Jiao Tong University, Shanghai, 200240, China

**Corresponding author: yetong@sjtu.edu.cn*

Abstract: This paper proposes a scheme for format conversion from a distorted non-return-to-zero (NRZ) signal to a high-quality return-to-zero (RZ) signal, using the nonlinearity in a coupled ring-resonator optical waveguide (CROW) on a silicon chip. In this method, a distorted NRZ signal is amplified and fed into the CROW together with an RZ pulse train. The CROW performs as a nonlinear step gate for the RZ pulse train, which outputs amplitude-equalized RZ pulses inheriting the information from the NRZ signal. Clearly, the integration of the format conversion and regeneration simplifies the system. Our simulations performed at 10 Gb/s and 40 Gb/s verify the feasibility of our proposal.

OCIS codes: (060.4510) Optic communication; (070.4340) Nonlinear optical signal processing; (230.1150) All-optical devices.

References and links

1. J. Wang, J. Sun, and Q. Sun, "Proposal for all-optical format conversion based on a periodically poled lithium niobate loop mirror," Opt. Lett. **32,** 1477 (2007).
2. C. H. Kwok and C. Lin, "Polarization-insensitive all-optical NRZ-to-RZ format conversion by spectral filtering of a cross phase modulation broadened signal spectrum," IEEE J. Sel. Top. Quantum Electron. **12,** 451 (2006).
3. C. G. Lee, Y. J. Kim, C. S. Park, H. J. Lee, and C.-S. Park, "Experimental demonstration of 10-Gb/s data format conversions between NRZ and RZ using SOA-loop-mirror," J. Lightwave Technol. **23,** 834 (2005).
4. J. Dong, X. Zhang, J. Xu, and D. Huang, "40 Gb/s all-optical NRZ to RZ format conversion using single SOA assisted by optical bandpass filter," Opt. Express **15**, 2907 (2007).
5. J. Yu, G. Chang, J. Barry, and Y. Su, "40 Gbit/s signal format conversion form NRZ to RZ using a Mach-Zehnder delay interferometer", Opt. Commum. **248,** 419 (2005).
6. C. Yan, Y. Su, L. Yi, L. Leng, X. Tian, X. Xu, and Y. Tian, "All-optical format conversion from NRZ to BPSK using a single saturated SOA," IEEE Photon. Technol. Lett. **18,** 2368 (2006).
7. W. Astar and G. M. Carter, "10 Gbit/s RZ-OOK to BPSK format conversion by cross-phase modulation in single semiconductor optical amplifier," Electron. Lett. **44,** (2008).
8. H. Jiang, H. Wen, L. Han, Y. Guo, and H. Zhang, "All-optical NRZ-OOK to BPSK format conversion in an SOA-based nonlinear polarization switch," IEEE Photon. Technol. Lett. **19,** 1985 (2007).
9. Y. Lu, F. Liu, M. Qiu, and Y. Su, "All-optical format conversions from NRZ to BPSK and QPSK based on nonlinear responses in silicon microring resonators," Opt. Lett. **15,** 14275 (2007).
10. B. E. Little, S. T. Chu, H. A. Haus, J. Foresi, and J.-P. Laine, "Microring resonator channel dropping filters," J. Lightwave Technol. **15,** 998 (1997).
11. M. A. Popović, T. Barwicz, M. R. Watt, P. T. Rakich, L. Socci, E. P. Ippen, F. X. Körtner, and H. I. Smith, "Multistage high-order microring-resonator filters with relaxed tolerances for high through-port extinction," in Proc. CLEO **1,** 266 (2005).
12. L. Ghişa, Y. Dumeige, N. N. T. Kim, Y. G. Boucher, and P. Féron, "Performances of a fully integrated all-optical pulse reshaper based on cascaded coupled nonlinear microring resonators," J. Lightwave Technol. **25,** 2417 (2007).

#96119 - $15.00 USD Received 16 May 2008; revised 4 Jul 2008; accepted 9 Jul 2008; published 15 Sep 2008

13. C. Manolatou and M. Lipson, "All-optical silicon modulators based on carrier injection by two-photon absorption," J. Lightwave Technol. **24,** 1433 (2006).
14. M. Waldow, T. Plötzing, M. Gottheil, M. Först, J. Bolten, T. Wahlbrink, and H. Kurz, "25 ps all-optical switching in oxygen implanted silicon-on-insulator microring resonator," Opt. Express **16,** 7693 (2008).
15. J. Niehusmann, A. Vörckel, P. H. Bolivar, T. Wahlbrink, W. Henschel, and H. Kurz, "Ultrahigh-quality-factor silicon-on-insulator microring resonator," Opt. Lett. **29,** 2861 (2004).
16. R. Salem, M. A. Foster, A. C. Turner, D. F. Geraghty, M. Lipson, and A. L. Gaeta, "All-optical regeneration on a silicon chip," Opt. Express **15,** 7802 (2007).
17. Q. Xu and M. Lipson, "Carrier-induced optical bistability in silicon ring resonators," Opt. Lett. **31,** 341 (2006).

1. Introduction

In the past few years, there has been an increasing interest in all-optical format conversion as it may become an important technology for future optical networks, which could employ various formats according to their scales and applications. Many schemes have been demonstrated to perform different types of format conversions, such as non-return-to-zero (NRZ)-to-return-to-zero (RZ) [1–5] and NRZ-to-phase-shift-keying (PSK) [6–9] conversions. All these proposals are based on an assumption that the input signal is of high quality. However, in practice, the signals to be converted are typically distorted due to the transmission over a certain distance. Therefore, the previous methods may not work very well, if the signal is seriously distorted after transmission.

To address this issue, this paper proposes a scheme to perform the format conversion from the distorted NRZ to a high-quality RZ signal, using a coupled ring-resonator optical waveguide (CROW) on a silicon chip. When the amplified NRZ signal is fed to the CROW together with an RZ pulse train, the CROW serves as a nonlinear step gate for the RZ pulses, which outputs an amplitude-equalized RZ signal inheriting the information from the NRZ signal. As a result, the signal quality is improved after the format conversion, which is thus called regenerative format conversion. Furthermore, such silicon converter possesses an advantage in its compatibility with the mature CMOS fabrication process, which makes the converter easy for high-density integration.

2. Principle

The proposed regenerative NRZ-to-RZ converter given in Fig. 1 consists of a chain of N-coupled microring resonators. These microrings have the same radius and are side-coupled to two straight waveguides. This structure is known as an N-order CROW. For example, the 3-order CROW in Fig. 3 contains 3 microrings and 4 coupling regions marked by the numbers '0', '1', '2', and '3', respectively, in the figure. By properly choosing the $N+1$ coupling coef-

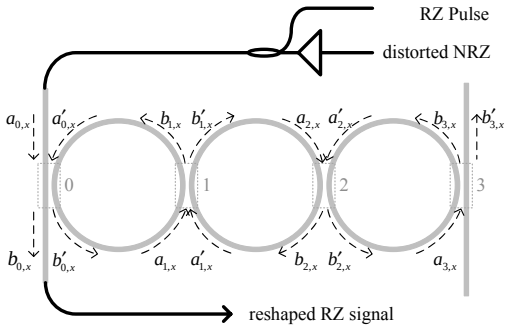

Fig. 1. Regenerative NRZ-to-RZ format converter using a single-stage silicon CROW.

#96119 - $15.00 USD Received 16 May 2008; revised 4 Jul 2008; accepted 9 Jul 2008; published 15 Sep 2008

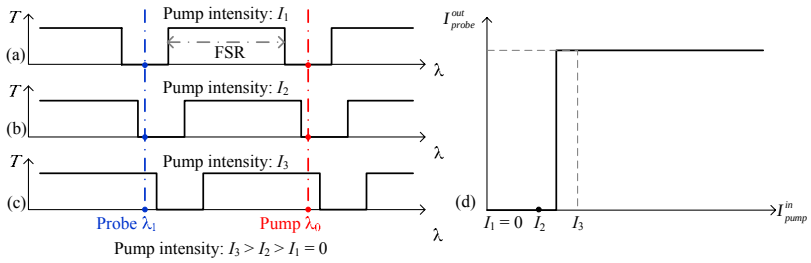

Fig. 2. Resonance shift increases with the increasing input pump power: (a) the pump power is zero; (b) the pump power is sufficiently small; (c) the pump power is sufficiently high; and (d) a nonlinear gate function for the probe light.

ficients, the CROW can exhibit a boxlike notch around its resonance wavelength [10], as displayed in Fig. 2. With the increasing of N, the filter response will be more boxlike. In practice, it is not easy to control all the parameters, such as the radii and coupling coefficients, precisely during the fabrication, which will induce an unexpectable modification on the notch shape. Fortunately, such mismatch can be post-compensated by a technique developed in Ref. [11], which is to modify the radius of the central ring using e-beam. Hence, we assume that the CROW can be fabricated as desired, following the process in [11]. When a high-power signal is injected into the CROW, the Kerr effect will cause a red shift of the resonance [12], as shown in Fig. 2. The shift increases with the increasing of the signal intensity. Based on this effect, Ref. [12] performed RZ signal reshaping using two cascaded CROWs. In this paper, we will show that the regenerative NRZ-to-RZ conversion can be achieved by a single CROW.

In Fig. 1, an amplified distorted NRZ at a wavelength λ_0 and a weak RZ pulse train at λ_1, which are used as pump and probe lights respectively, are fed into the CROW simultaneously. In our scheme, both λ_0 and λ_1 are set at the resonance wavelengths to maximize the power coupling to the microrings. Assume that the probe light is weak enough such that the resonance shift is solely determined by the pump intensity. For the input of distorted '0' bits, though there is a small fluctuation in power, the pump power is sufficiently weak, which induces a little shift of the resonance. Due to the boxlike filtering effect of the CROW at the resonance, the RZ signal still lies in the bottom of the notch, as illustrated in Fig. 2(b). In this case, the CROW has no output at λ_1. When the pump input is a distorted '1' bit, the pump power becomes very high, such that it makes the resonance wavelength shift significantly and the RZ signal is completely off-resonance in Fig. 2(c). In this case, the transferred intensity of the RZ pulse is maximized. As a result, the CROW provides the RZ pulse train a gate transfer function in Fig. 2(d), with the help of the boxlike notch effect.

To explore the intrinsic mechanism of the proposed scheme, we extend the model in Ref. [9] and [12] to delineate the process that the probe light interacts with the pump light in the CROW. Let $a_{i,0}$ and $a'_{i,0}$ ($a_{i,1}$ and $a'_{i,1}$) be the input fields of the pump (probe) light in i-th coupling region, and $b_{i,0}$ and $b'_{i,0}$ ($b_{i,1}$ and $b'_{i,1}$) be the output fields of the pump (probe) light, as shown in Fig. 1. In the i-th coupling region, there is:

$$\begin{bmatrix} b_{i,x} \\ b'_{i,x} \end{bmatrix} = \begin{bmatrix} t_i & j\sigma_i \\ j\sigma_i & t_i \end{bmatrix} \begin{bmatrix} a_{i,x} \\ a'_{i,x} \end{bmatrix}, \quad x = 0,1 \text{ and } i \in \{0,1,\cdots,N\}$$

where the self- (t_i) and cross-coupling (σ_i) coefficients are related by $t_i^2 + \sigma_i^2 = 1$. Then we

#96119 - $15.00 USD Received 16 May 2008; revised 4 Jul 2008; accepted 9 Jul 2008; published 15 Sep 2008

have:

$$\begin{bmatrix} a_{i,x} \\ b_{i,x} \end{bmatrix} = \begin{bmatrix} j\frac{t_i}{\sigma_i} & -j\frac{1}{\sigma_i} \\ j\frac{1}{\sigma_i} & -j\frac{t_i}{\sigma_i} \end{bmatrix} \begin{bmatrix} a'_{i,x} \\ b'_{i,x} \end{bmatrix}, \quad x = 1,2. \tag{1}$$

When the lights are travelling in the waveguide, both the phases of the pump and probe lights are modulated by the intensity of the pump light due to Kerr effect, which can be described by solving nonlinear Schrödinger equation [9]. For the pump light, $a'_{i,0}$ ($a_{i+1,0}$) is related to $b_{i+1,0}$ ($b'_{i,0}$) by [12]:

$$\begin{cases} a'_{i,0} = b_{i+1,0} \exp\left(\frac{\alpha}{2}L\right) \exp\left[-jk_0L - j\gamma_0|b_{i+1,0}|^2\right] \\ b'_{i,0} = a_{i+1,0} \exp\left(-\frac{\alpha}{2}L\right) \exp\left[jk_0L + j\frac{\gamma_0|a_{i+1,0}|^2}{e^{\alpha L}}\right] \end{cases}, \tag{2}$$

where α is the linear loss coefficient, $k_0 = 2\pi n_e/\lambda_0$ is the propagation constant, n_e is the effective index, L is the half-perimeter of the rings, n_2 is the nonlinear refractive index, and γ_0 characterizes the nonlinear properties

$$\gamma_0 = \frac{\pi n_2 \varepsilon_0 c n_e}{\lambda_0} \frac{e^{\alpha L} - 1}{\alpha}.$$

Similarly, we can find the following relationship for the probe light:

$$\begin{cases} a'_{i,1} = b_{i+1,1} \exp\left(\frac{\alpha}{2}L\right) \exp\left[-jk_1L - j2\gamma_1|b_{i+1,0}|^2\right] \\ b'_{i,1} = a_{i+1,1} \exp\left(-\frac{\alpha}{2}L\right) \exp\left[jk_1L + j\frac{2\gamma_1|a_{i+1,0}|^2}{e^{\alpha L}}\right] \end{cases}, \tag{3}$$

where

$$k_1 = \frac{2\pi n_e}{\lambda_1} \text{ and } \gamma_1 = \frac{\pi n_2 \varepsilon_0 c n_e}{\lambda_1} \frac{e^{\alpha L} - 1}{\alpha}.$$

By numerically solving Eqs. (1)-(3), one can obtain $b_{0,x}$ from $a_{0,x}$ in the steady state. Note that, in the above model, the optical loss induced by two-photon absorption (TPA) [13] is neglected for simplicity. However, the TPA will happen if two lights around 1550 nm are injected into a silicon waveguide simultaneously. Meanwhile, the free carrier generated during the TPA process will cause a change in the refractive index [13] opposite to the Kerr effect. Fortunately, the oxygen ion implantation technique introduced in [14] can already reduce the carrier lifetime to 15 ps. In our calculation and simulation, we take the TPA absorption into account while ignore the index change induced by the free carriers.

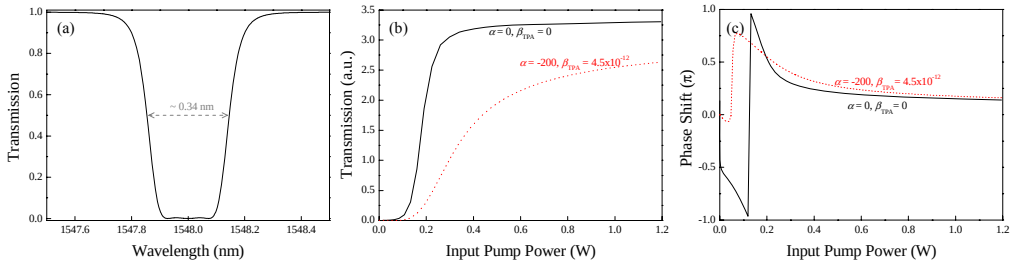

Fig. 3. (a) linear and (b) nonlinear effects of the 3-ring silicon CROW.

#96119 - $15.00 USD Received 16 May 2008; revised 4 Jul 2008; accepted 9 Jul 2008; published 15 Sep 2008

3. Simulation results

In this paper, we employ a silicon CROW containing 3 rings, where the radius of each ring $R \approx 18$ μm and the cross-sectional dimensions of the waveguide is 450 nm $\times$ 250 nm. The effective index of nano-scale silicon waveguides is $n_e \approx 2.5$. The free spectral range (FSR) of the CROW is about 8.55 nm. By setting the cross-coupling coefficients $\sigma_0 = \sigma_3 = 0.4$ and $\sigma_1 = \sigma_2 = 0.072$, the CROW can exhibit a boxlike notch at its resonant wavelength of 1548 nm, as plotted in Fig. 3(a). We set the pump light at 1548 nm, and the probe light at another resonant wavelength of 1539.45 nm, which is phase modulated by the pump light due to the Kerr effect. Typically, for silicon waveguides, the nonlinear index $n_2 \approx 7.9 \times 10^{-18}$ m^2/W and the TPA coefficient $\beta_{TPA} = 4.5 \times 10^{-12}$ m/W around 1550 nm [13]. Assuming the linear loss coefficient $\alpha \approx -200$ dB/m [15], Fig. 3(b) displays the output probe power changing with the input pump power in the steady state, with and without optical losses. It shows a sharp step gate in the lossless case, which is however flattened by the optical losses. Similarly, in Fig. 3(c), the probe phase has an abrupt transition with the increase of the pump power. For example, in the lossless case, the probe phase is in the range of $-0.5\pi \sim -\pi$ when the pump power is less than 0.05 W, while approaches to 0.2π when the pump power is larger than 0.4 W.

To verify the feasibility of our proposal, we simulate the dynamic case using finite difference method [12]. We generate a 10-Gb/s optical NRZ signal using a $2^7 - 1$ pseudo-random binary sequence (PRBS), and transmit it over a standard single mode fiber (SMF) without any dispersion compensation. The eye-diagrams of the NRZ signals after 20-km transmissions are given in Fig. 4(a). We feed the distorted signals after amplification together with a weak 20%-duty-cycle RZ pulse train to the CROW. Figure 4(d) is the spectrum of the RZ pulse train, which has a 3-dB bandwidth of $\sim$ 36 GHz. Figures 4(b) and 4(c) display the RZ signals after format conversion using the CROW without and with taking the optical losses into consideration. Improvement of the eye-opening confirms that the signal quality is remarkably improved after the format conversion. Our simulation results further show that, to get the same signal quality, a

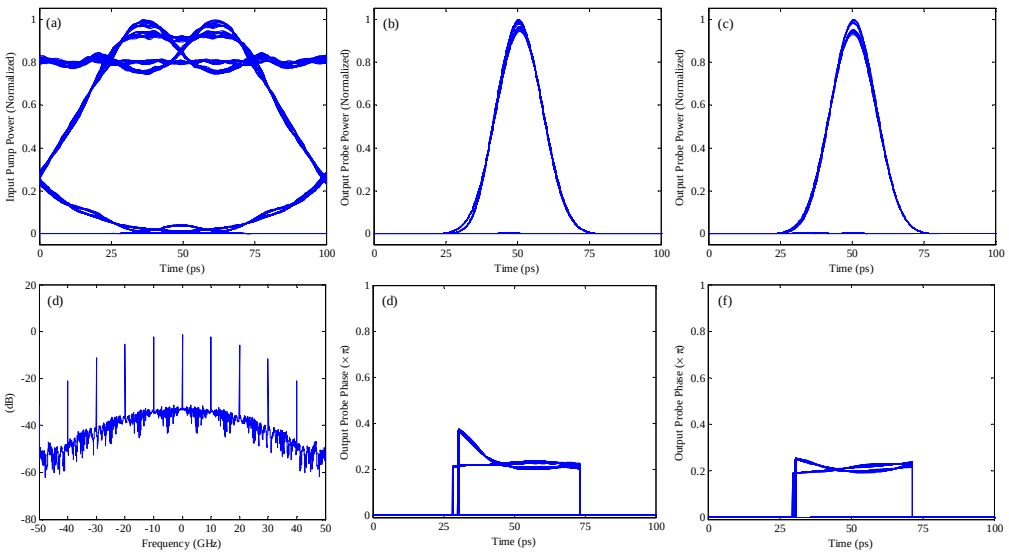

Fig. 4. 10-Gb/s regenerative NRZ-to-RZ format conversion: (a) NRZ signals after 20-km transmission without any compensation; (b), (e) RZ signal after conversion in lossless case; (c), (f) RZ signals after conversion in the presence of optical losses; (d) spectral of the input 10-GHz RZ pulse train.

#96119 - $15.00 USD Received 16 May 2008; revised 4 Jul 2008; accepted 9 Jul 2008; published 15 Sep 2008

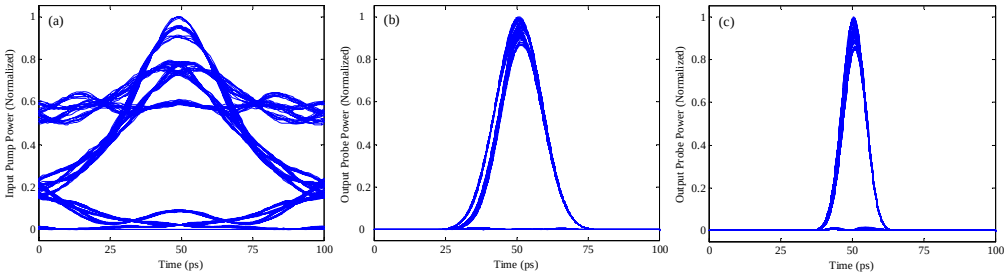

Fig. 5. 10-Gb/s regenerative NRZ-to-RZ format conversion in the presence of optical losses, where the peak pump power is about 1.1 W: (a) NRZ signals after 40-km transmission without any compensation; (b) 20%-duty-cycle, and (c) 10%-duty-cycle RZ signal after conversion.

higher peak pump power is required if the optical losses in the CROW can not be ignored, since the nonlinear step gate is flattened by the optical losses. For example, to achieve the RZ signal in Fig. 4(b), we inject an NRZ signal with a peak power of 530 mW to the CROW, while, to obtain the signal in Fig. 4(c), the input NRZ signal should be amplified to have a peak power of 897 mW. This result indicates that, though the Kerr effect is widely believed to perform ultra-fast optical signal processing, it requires a very high pump power. Another example is that, Ref. [16] experimentally demonstrated signal regeneration based on the self-phase modulation (SPM) in the silicon waveguide, where the pump power is up to 6 W. Note that, with a high input power, the nonlinear performance of the silicon microring resonator is affected by the thermal optical effect, which is relatively slow (microsecond transition time) and can be ignored when the input pulse width is short (less than tens of nanoseconds) [17].

We investigate the chirp of the converted signal in Figs. 4(e)-4(f), which provide the phase eye-diagrams corresponding to the results in Figs. 4(b) and 4(c). Note that, we do not consider the phase of bit '0' in Figs. 4(e) and 4(f) since the amplitude of bit '0' is close to zero and thus the chirp can be ignored. As predicted by Fig. 3(c), the converted signals do not exhibit severe chirp, and the phase of the pulse almost varies around 0.2π, especially in the lossy case where the power of bit '1' changes between 670 mW and 890 mW.

We perform regenerative conversion for the 10-Gb/s NRZ signal after 40-km transmission without any compensation. Due to the chromatic dispersion, a significant broadening of the NRZ signal can be observed in Fig. 5(a). Both amplitude fluctuations on bit '0' and '1' are severer than that in Fig. 4(a). Again, after the CROW, we can obtain a clean RZ signal in Fig. 5(b). However, the eye-diagram exhibits timing jitter, which is essentially a kind of pattern effect. When the input NRZ signal is a string of consecutive '1' bits, the pump power keeps at a high level, and the CROW outputs a sequence of RZ pulses without any delay. However, when the input signal is in a transition from '0' to '1', there is a flat and long rising edge ($\sim$ 100 ps) induced by the severe dispersion. At the rising edge, the pump power increases slowly from a low level to a high level, which consequently postpones the output of the RZ pulses. Therefore, in Fig. 5(b), we can see double edges on the left. One possible way to alleviate the timing jitter is to reduce the duty cycle of the RZ pulse train such that the rising process is completed before the RZ pulse is injected to the CROW. For example, if we use a 10%-duty-cycle RZ pulse train, the timing jitter can be suppressed in Fig. 5(c).

This scheme can also perform regenerative NRZ-to-RZ conversion at a higher data-rate, for example 40 Gb/s. To confirm this, a 10-dBm NRZ signal is generated and transmitted over a 40-km fiber. After chromatic dispersion compensation, the signal is impaired by fiber nonlinearity, as plotted in Fig. 6(a). To carry out the conversion for the 40-Gb/s NRZ data, we use a CROW

#96119 - $15.00 USD Received 16 May 2008; revised 4 Jul 2008; accepted 9 Jul 2008; published 15 Sep 2008

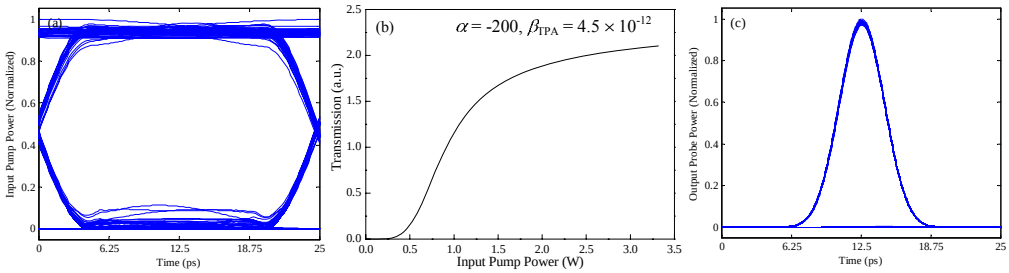

Fig. 6. 40-Gb/s regenerative NRZ-to-RZ format conversion: (a) NRZ signals after 40-km transmission with chromatic dispersion compensation; (b) RZ signal after conversion with the presence of optical losses.

with a 3-dB bandwidth of ~ 1 nm, where the coupling coefficients are $\sigma_0 = \sigma_3 = 0.52$ and $\sigma_1 = \sigma_2 = 0.13$ [12]. The transmission characteristic of the CROW is given in Fig. 6(b), where the curve becomes saturated when the pump power is larger than 1.8 W. Therefore, the NRZ signal is amplified such that its peak power reaches 2 W. The input 40-GHz RZ pulses with a duty cycle of 20% show a 3-dB bandwidth of ~ 120 GHz in the spectrum. By using the proposed method, the distorted signal is converted to a 40-Gb/s RZ signal in Fig. 6(b). Again, it is shown that the fluctuation in amplitude and time-jitter of the signal are significantly suppressed after the format conversion.

4. Conclusion

In summary, we have proposed a new technique to convert a distorted NRZ signal to a high-quality RZ signal, using the nonlinear effects in a silicon CROW structure. The scheme has the advantages including simplicity, high speed, and high density integration. Our simulations performed at 10 Gb/s and 40 Gb/s demonstrate the feasibility of our proposal.

Acknowledgments

This work was supported by the SJTU Young Faculty Foundation (A92828) and the NSFC (60777040).

#96119 - $15.00 USD Received 16 May 2008; revised 4 Jul 2008; accepted 9 Jul 2008; published 15 Sep 2008